Supporting Information

Electron Transfer Initiated Formation of Covalently Bound Organic Layers on Silicon Surfaces

Kallum M. Koczkur, Emad M. Hamed, M'hamed Chahma, Daniel F. Thomas and Abdelaziz Houmam*

*To whom correspondence should be addressed: ahoumam@uoguelph.ca

I. Multilayer formation on a surface from aryl diazonium salts

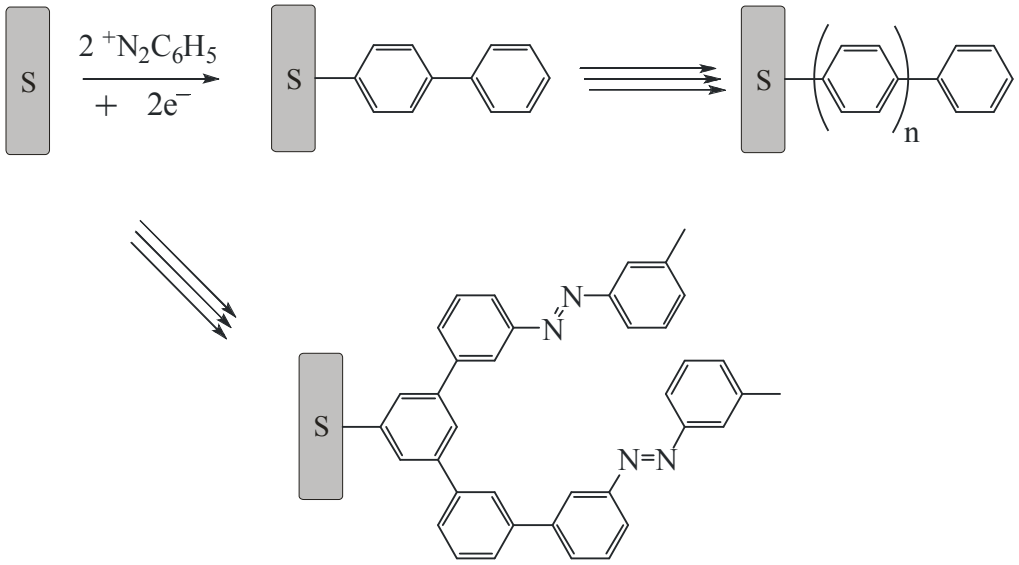

Scheme S1. Multilayer formation on a surface from an aryl diazonium salt.[1]

II. Theoretical calculations

Theoretical calculations were performed using the Gaussian 09 software package.[1] Optimized structures for the $Si_{17}H_{24}$ cluster, meant to simulate a hydrogen terminated Si(111) surface, and the $Si_{17}H_{22}$ NBS cluster were calculated using the B3LYP method[2] with the 6-311G+(d,p) basis set. The method, basis set and silicon cluster size were chosen based on the results of a recently published paper.[3] We checked that the obtained confirmations were real minima by running frequency calculations for the B3LYP calculations. No imaginary frequencies were observed. During the two cluster calculations, subsurface atoms were not held in a fixed position. Further calculations were not undertaken in the present study beyond the attachment of the succidimyl group and bromine atom to the Si(111) surface due to the uncertainly of the experimental surface structure. These calculations do show however, that existence of a succidimyl group and bromine atom on neighbouring surface sites on the Si(111) surface is theoretically possible.

$Si_{17}H_{24}$ Cluster

Total Energy: -4936.40670565 a.u.

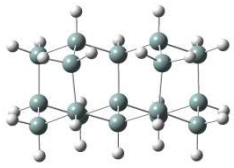

Center Number	Atomic Number	Atomic Type	Coordinates (Angstroms) X	Y	Z
1	14	0	-1.930216	1.993291	-1.297858
2	1	0	-3.148844	2.008310	-2.160567
3	14	0	-1.900961	0.000000	-0.011823
4	1	0	-3.127586	0.000000	0.841913
5	14	0	-1.930216	-1.993291	-1.297858
6	1	0	-3.148844	-2.008310	-2.160567
7	14	0	0.000000	2.210714	-2.646836
8	1	0	0.000000	1.215704	-3.752016
9	1	0	0.000000	3.570073	-3.259273
10	14	0	0.000000	-2.210714	-2.646836
11	1	0	0.000000	-1.215704	-3.752016
12	1	0	0.000000	-3.570073	-3.259273
13	14	0	-1.957941	-3.869273	0.146029
14	1	0	-3.152080	-3.822546	1.036197
15	1	0	-2.042207	-5.116435	-0.665835
16	14	0	-1.957941	3.869273	0.146029
17	1	0	-2.042207	5.116435	-0.665835
18	1	0	-3.152080	3.822546	1.036197

19	14	0	0.000000	3.884634	1.473323
20	1	0	0.000000	5.090532	2.353836
21	14	0	1.957941	3.869273	0.146029
22	1	0	2.042207	5.116435	-0.665835
23	1	0	3.152080	3.822546	1.036197
24	14	0	0.000000	1.924334	2.788331
25	1	0	1.203528	1.890391	3.667217
26	1	0	-1.203528	1.890391	3.667217
27	14	0	1.930216	1.993291	-1.297858
28	14	0	0.000000	0.000000	1.410114
29	14	0	0.000000	-1.924334	2.788331
30	1	0	-1.203528	-1.890391	3.667217
31	1	0	1.203528	-1.890391	3.667217
32	14	0	0.000000	-3.884634	1.473323
33	1	0	0.000000	-5.090532	2.353836
34	14	0	1.930216	-1.993291	-1.297858
35	14	0	1.900961	0.000000	-0.011823
36	1	0	3.127586	0.000000	0.841913
37	14	0	1.957941	-3.869273	0.146029
38	1	0	2.042207	-5.116435	-0.665835
39	1	0	3.152080	-3.822546	1.036197
40	1	0	3.148844	2.008310	-2.160567
41	1	0	3.148844	-2.008310	-2.160567

$Si_{17}H_{22}$ NBS Cluster

Total Energy: -7869.60185476 a.u.

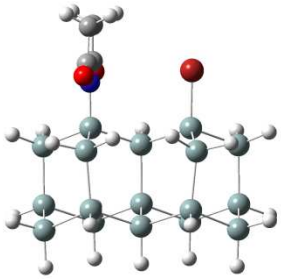

Center Number	Atomic Number	Atomic Type	Coordinates (Angstroms) X	Y	Z
1	14	0	2.175721	0.400312	-0.058019
2	14	0	0.158865	-0.314314	-1.094565
3	1	0	0.431788	-0.703997	-2.504743
4	14	0	-0.878847	-2.174379	-0.049697
5	14	0	1.838675	1.048581	2.196981
6	1	0	1.380519	-0.066511	3.056199
7	1	0	3.083075	1.651300	2.739547
8	14	0	-1.541502	-1.776647	2.183730
9	1	0	-0.365230	-1.668318	3.082669
10	1	0	-2.365061	-2.937204	2.624311
11	14	0	-2.825018	-2.785685	-1.249642
12	1	0	-2.478928	-3.076940	-2.667597
13	1	0	-3.399894	-4.015654	-0.638872
14	14	0	3.086200	2.259203	-1.213126

15	1	0	4.355189	2.647967	-0.533653
16	1	0	3.393815	1.918906	-2.626120
17	14	0	1.538603	4.049178	-1.144207
18	1	0	2.121223	5.220759	-1.863237
19	14	0	1.005181	4.639709	1.080434
20	1	0	2.221393	5.140114	1.781686
21	1	0	-0.003439	5.736572	1.071868
22	14	0	-0.441808	3.348050	-2.221038
23	1	0	-1.440638	4.454282	-2.237518
24	1	0	-0.162297	2.963431	-3.633059
25	14	0	0.169473	2.737929	2.209877
26	14	0	-1.388528	1.492498	-1.096072
27	14	0	-3.373781	0.862142	-2.222703
28	1	0	-3.050454	0.535532	-3.640047
29	1	0	-4.310699	2.021154	-2.222333
30	14	0	-4.369775	-0.992248	-1.156694
31	1	0	-5.621317	-1.389399	-1.867403
32	14	0	-2.883347	0.174267	2.221035
33	14	0	-1.837209	2.025530	1.169472
34	1	0	-2.814556	3.155514	1.199225
35	14	0	-4.877449	-0.375784	1.070327
36	1	0	-5.565917	-1.496103	1.771347
37	1	0	-5.803143	0.791365	1.048671
38	1	0	-0.130845	3.102560	3.627237
39	1	0	-3.201267	0.517255	3.638816
40	35	0	0.570011	-3.964836	-0.075739
41	6	0	3.772951	-1.599902	-1.289169
42	6	0	3.988716	-1.556413	1.022680
43	6	0	4.722569	-2.742928	-0.961205
44	6	0	4.868858	-2.710742	0.563123
45	1	0	4.284817	-3.669368	-1.338277
46	1	0	5.659726	-2.585369	-1.498629
47	1	0	4.522985	-3.621599	1.055817
48	1	0	5.889420	-2.526727	0.904910
49	7	0	3.375336	-0.976511	-0.095691
50	8	0	3.402016	-1.254791	-2.386191
51	8	0	3.835121	-1.181657	2.162688

$Si_{17}H_{22}$ NBP Cluster

Total Energy: -8022.06022721 a.u.

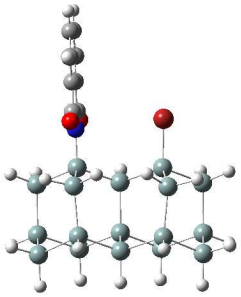

Center Number	Atomic Number	Atomic Type	Coordinates (Angstroms) X	Y	Z
1	14	0	1.297983	1.371319	-0.027023
2	14	0	-0.176772	-0.176839	-1.068717
3	1	0	0.271777	-0.424715	-2.466311
4	14	0	-0.319501	-2.293828	-0.004373
5	14	0	0.666528	1.815642	2.213425
6	1	0	0.754298	0.617024	3.078214
7	1	0	1.500252	2.914882	2.764898
8	14	0	-1.148829	-2.208495	2.207873
9	1	0	-0.168092	-1.574117	3.124457
10	1	0	-1.378707	-3.609093	2.660572
11	14	0	-1.768314	-3.704046	-1.235369
12	1	0	-1.291088	-3.820887	-2.640479
13	1	0	-1.759652	-5.058929	-0.618099
14	14	0	1.293194	3.441113	-1.185311
15	1	0	2.250665	4.352747	-0.495929
16	1	0	1.738487	3.272781	-2.593348
17	14	0	-0.886748	4.359258	-1.150172
18	1	0	-0.875989	5.668701	-1.867660
19	14	0	-1.667414	4.651024	1.060757
20	1	0	-0.819758	5.647900	1.774245
21	1	0	-3.061640	5.176030	1.026515
22	14	0	-2.319037	2.845723	-2.258014
23	1	0	-3.707166	3.386186	-2.310864
24	1	0	-1.861474	2.625377	-3.658901
25	14	0	-1.582721	2.576019	2.192128
26	14	0	-2.360859	0.764249	-1.129232
27	14	0	-3.840978	-0.679119	-2.283187
28	1	0	-3.371633	-0.838747	-3.688483
29	1	0	-5.190552	-0.047917	-2.320337
30	14	0	-3.947800	-2.777952	-1.209262
31	1	0	-4.876952	-3.689401	-1.940895
32	14	0	-3.218241	-1.057314	2.179583
33	14	0	-3.052149	1.057206	1.118739
34	1	0	-4.421430	1.655933	1.113329
35	14	0	-4.732229	-2.439004	0.996157
36	1	0	-4.867346	-3.744742	1.701697
37	1	0	-6.079376	-1.804943	0.940924
38	1	0	-2.035927	2.763891	3.603289
39	1	0	-3.696625	-0.877542	3.582499
40	6	0	3.812704	0.496870	1.092398
41	6	0	3.668823	0.327399	-1.216470

42	6	0	5.100412	-0.057551	0.585093
43	6	0	5.014290	-0.158809	-0.800309
44	6	0	6.245117	-0.433435	1.270660
45	6	0	6.068267	-0.641147	-1.560410
46	6	0	7.314271	-0.922456	0.513957
47	1	0	6.302846	-0.350790	2.349189
48	6	0	7.227322	-1.024607	-0.879130
49	1	0	5.990834	-0.716310	-2.638277
50	1	0	8.226934	-1.228511	1.012245
51	1	0	8.073990	-1.408075	-1.436845
52	35	0	1.763443	-3.262349	0.030217
53	8	0	3.207183	0.409689	-2.331130
54	8	0	3.504898	0.741743	2.237199
55	7	0	2.989053	0.705294	-0.035505

References

(1) Frisch, M. J.; Trucks, G. W.; Schlegel, H. B.; Scuseria, G. E.; Robb, M. A.; Cheeseman, J. R.; Scalmani, G.; Barone, V.; Mennucci, B.; Petersson, G. A.; Nakatsuji, H.; Caricato, M.; Li, X.; Hratchian, H. P.; Izmaylov, A. F.; Bloino, J.; Zheng, G.; Sonnenberg, J. L.; Hada, M.; Ehara, M.; Toyota, K.; Fukuda, R.; Hasegawa, J.; Ishida, M.; Nakajima, T.; Honda, Y.; Kitao, O.; Nakai, H.; Vreven, T.; Montgomery Jr., J. A.; Peralta, J. E.; Ogliaro, F.; Bearpark, M.; Heyd, J. J.; Brothers, E.; Kudin, K. N.; Staroverov, V. N.; Keith, T.; Kobayashi, R.; Normand, J.; Raghavachari, K.; Rendell, A.; Burant, J. C.; Iyengar, S. S.; Tomasi, J.; Cossi, M.; Rega, N.; Millam, J. M.; Klene, M.; Knox, J. E.; Cross, J. B.; Bakken, V.; Adamo, C.; Jaramillo, J.; Gomperts, R.; Stratmann, R. E.; Yazyev, O.; Austin, A. J.; Cammi, R.; Pomelli, C.; Ochterski, J. W.; Martin, R. L.; Morokuma, K.; Zakrzewski, V. G.; Voth, G. A.; Salvador, P.; Dannenberg, J. J.; Dapprich, S.; Daniels, A. D.; Farkas, O.; Foresman, J. B.; Ortiz, J. V.; Cioslowski, J.; Fox, D. J. Gaussian 09, Revision D.01, Gaussian, Inc., Wallingford CT, **2013**.

(2) Becke, A. D. A new mixing of Hartree-Fock and local density-functional theories. *J. Chem. Phys.* **1993**, *98*, 1372-1377.

(3) Tian, F.; Cui, Y.; Teplyakov, A. V. Nitroxidation of H-Terminated Si(111) Surfaces with Nitrobenzene and Nitrosobenzene. *J. Phys. Chem. C* **2014**, *118*, 502-512.

III. IRRAS data

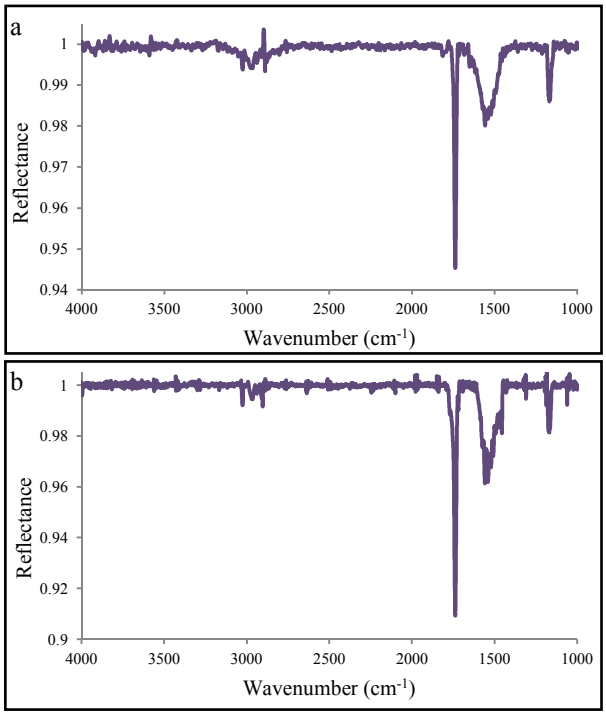

Figure S1. IRRAS data for Si(111) modified with (a) NBS/Fc followed by treatment with a succinimidyl anion.

IV. Line profile details

- The line profile shown in Figure 3d (in the manuscript) is taken (on purpose) in the perpendicular direction of the descending steps (in Figure 3c) to minimize the effect of the steps in deducing an average thickness. So the 10 steps observed in Figure 3c should not be expected in the line profile (Figure 3d).

- The size of the image in Figure 3c is only 0.8x0.8 μm^2 while that of the image in Figure 3b is 3x3 μm^2. When the whole scratched area is scanned the resolution is lost.

- The line profile in Figure 3d does indeed show silicon steps as can be seen in the line profile below (Figure S2. This is the same line profile reported in Figure 3d that has just been expended).

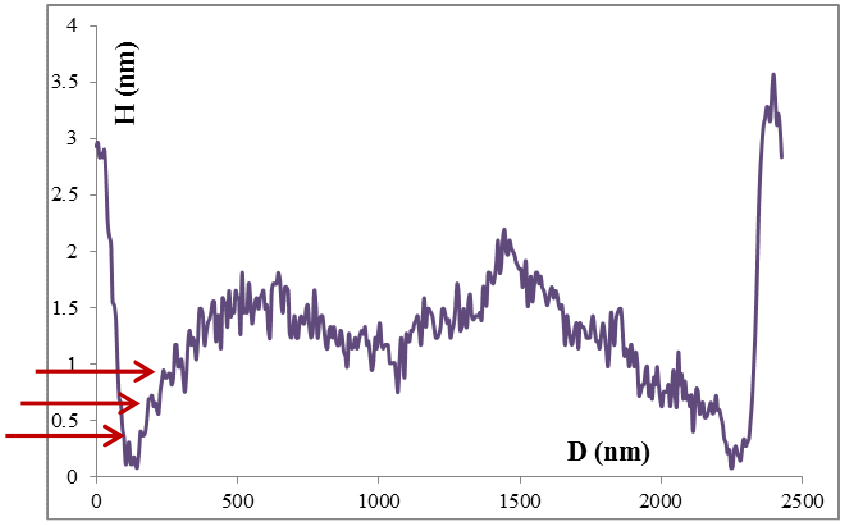

Figure S2. Representative line profile illustrating the approximate depth of the multilayers.

V. Comparison of the XPS Si 2p signal for a modified Si(111) surface and an oxidize Si(111) surface

The Si signal shows certainly the attachment of other elements in addition to O. The Figure below shows the Si 2p signal for an oxidized Si surface (a) and a Si surface modified using the bromosuccinimide / ferrocene mixture (b and c). The modified surface does show the signal observed for the oxidized surface but does also show other signals. The assignments are done in accordance with those reported in the literature to the best of our ability. Br, N and O (from the carbonyl groups of the succinimidyl) can all be attached to Si in the present work, given their potential involvement in radical reactions.

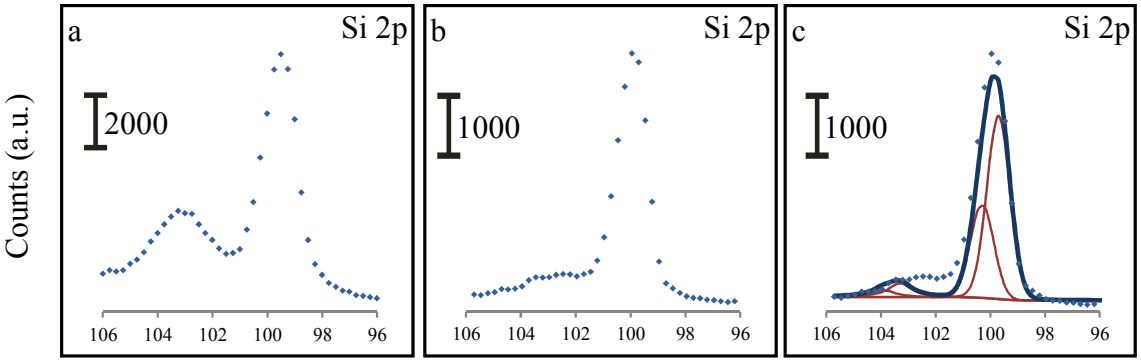

Figure S3. XPS spectra of (a) Si(111) with an oxide layer, (b) Si(111)-H modified with NBS/Fc and (c) Si(111)-H modified with NBS/Fc with peak fitting for the bulk silicon signal and silicon oxide signal. These spectra show differences in signal intensity due to surface modification and (c) suggests that more than more species are present on the surface in addition to silicon oxide.